Supplementary Table 1. Oligonucleotide primers used in this study.

oBB #	Primer Name	Nucleotide Seq. (5'-3')	Length	Tm	GC%	Product Size (bp)
csp1 genotyping primers (followed by HindIII digestion)						
196	Prdm16_i6-7_F4	GGGATCACCTAACAAGTGATGATT	24	60.47	41.67	494
197	Prdm16_i6-7_R4	TCTAATCCACCACACCTCATCTC	23	60.38	47.83	494
csp1 recombinant interval - genotyping microsatellite markers						
96	chr4TG_375328F	CCAGCTTGGGTGAATCTGTT	20	60.11	50	168
97	chr4TG_375328R	CGGCCTCAGAGATCAGAAAC	20	59.95	55	168
120	chr4complex_920386F	GACCTGAAGGCTGCCATAAC	20	59.7	55	180
121	chr4complex_920386R	AGGACTCAAGCAAACTGGACA	21	59.9	47.62	180
Novel microsatellite markers for *csp1* fine-mapping						
1	chr4(CA)n_2097975_F	AGGCCTCCTAGAAGGACAGC	20	59.98	60	204
2	chr4(CA)n_2097975_R	AGCCCAGATACTGCAAGCTC	20	59.6	55	204
5	chr4(CA)n_1052954_F	CTGCTAAAACTTACAAAGGTGGACT	25	59.36	40	400
6	chr4(CA)n_1052954_R	GCTACCTCCTTTCCTTTTGTGA	22	59.76	45.45	400
130	chr4CA_1275257F	GACCATGCCACTGCACTTC	19	60.27	57.89	190
131	chr4CA_1275257R	GGGAAGAGAAGGTGTGTCCA	20	60.09	55	190
MIT microsatellite markers for *csp1* fine-mapping						
	D4Mit13					
	D4Mit42					
	D4Mit254					
	D4Mit344					
	D4Mit256					
Prdm16 in situ probe primers						
164	Prdm16x4-8F	CTGGCTCAAGTACATCCGTGT	21	60.19	52.38	649
165	Prdm16x4-8R	CGTGCTGTGGATATGCTTGT	20	59.75	50	649
381	Prdm16-3'UTR-F	CACCCTCAACACCTCCACTT	20	59.99	55	504
382	Prdm16-3'UTR-R	AGGTGTGGGTTTGCCAATAA	20	60.23	45	504

PRDM16 cDNA primers for anibody generation						
214	Prdm16-Nterm-F	GAATTCAGGCGAGGGCGAGGAAG	23	63.98	70.59	175
215	Prdm16-Nterm-R	AAGCTTGGAGTGAAGTCCTCGCTGGTG	27	64.56	61.9	175
216	Prdm16-mid-F	GAATTCATTACACGCCTGGCAGCATC	26	63.42	55	685
217	Prdm16-mid-R	AAGCTTGGTGGCGGGAAGAAGGAAT	25	63.54	57.89	685
Prdm16 FL and S cDNA amplification Primers						
972	Prdm16FL-5'F	CACCATGCGATCCAAGGCGAGGGCGA	26	ND	65.3	NA
538	Prdm16FL-3'R	GAGGTGGTTGATGGGGTTAAAGGCT	25	68.12	52.0	NA
1053	Prdm16S-x4ATG_F	CACCATGTGTCAGATCAACGAACAGAT	27	55.89	44.4	NA
1034	Prdm16cpo1-3'R	CCGTGCTGTGGATATGCTTGTGCTGTTTG	29	74.69	51.72	NA

LEGENDS TO SUPPLEMENTARY FIGURES

Supplemental Figure 1. *csp1* mutant palate shelves can fuse in the absence of the mandible and tongue. wild-type (**A**) and *csp1* homozygous mutants (**B**) show palate shelf elevation, apposition and fusion in the absence of the mandible and tongue after approximately three days of *in vitro* suspension palate culture. Histologic examination of Hematoxylin and Eosin-stained coronal sections through the cultured palate shelves show that complete fusion of the bilateral palate shelves at the midline in wild-type (**C**) and *csp1* mutant (**D**) embryos showing complete fusion upon gross examination. Detailed compilation of suspension palate culture results is provided in the accompanying table.

Supplemental Figure 2. *Prdm16* expression during embryonic limb formation. *Prdm16* expression appears at about E10.5 and is robust in the mesenchyme of the forelimb and hindlimb buds by E11.5 (**A**). *Prdm16* expression becomes gradually more restricted to the condensing cartilage of the future digits at E12.5 (**B**) and gradually becomes refined to the regions surrounding the sites of future joint formation in the digits of the forelimb (**C** and **D**), hindlimbs (**E**) and knee (black arrowhead in **F**) from E13.5-E15.5.

Supplemental Figure 3. The *Prdm16*^{Gt683Lex} mutation causes recessive CP, and reporter expression in craniofacial structures is consistent with this phenotype. (**A**-**P**) Histological analysis of coronal sections through the posterior (**A, E, V, M),** medial (**B, F, J, N)** and anterior (**C, G, K, O)** aspects of the secondary palate in heterozygous control and homozygous *Prdm16*^{Gt683Lex} E13.5 and E14.5 embryos. Reporter expression is dose-sensitive. (**A-H**) At E13.5,

before palate shelf elevation and fusion, *Prdm16* reporter expression is strongest in the mesenchyme at the oral side of the palate shelves, although it is visible throughout the palate shelf and hinge region. Expression within the tongue musculature, molar tooth mesenchyme, and within Meckel's cartilage and surrounding perichondrium is also detected. Low-level expression in palate epithelia is difficult to visualize. (**I-P**) This expression pattern is maintained at E14.5, after palate shelf elevation and fusion. (**A-D, V-L**) The most intense palatal *Prdm16* expression is evident on the oral side of the palate shelves, while a posterior-anterior gradient of increased expression is evident in the palate shelves through to the highest expression in the primary palate and upper incisor regions (**D, H, L, P**). V (Trigeminal ganglion), ps (palate shelf), T (tongue), MC (Meckel's cartilage), m (molar), i (incisor), pp (primary palate).

Supplemental Figure 4. Loss of *Prdm16* expression perturbs *in vivo* TGFβ signaling in the mandible. Immunofluorescent detection of TGFβ2, TGFβ3, Phospho-SMAD2, Phospho-SMAD1, 5, 8 and SMAD7 protein expression in wild-type (*wt*) (**A-F, J-M**) versus $Prdm16^{Gt683Lex}$ gene trap null mutant (*gt*) (**G-I, N, O**) E13.5 embryos. Expression of each protein in wild-type embryos is evident in secondary palate shelves, tongue, Meckel's cartilage, molar teeth and the undifferentiated mesenchyme betweend the oral sulci at the sides of the tongue and the perichodrium surrounding Meckel's cartilage which contains the salivary ducts (**A-F, J-M**). A dramatic reduction in protein expression levels for each protein is observed in $Prdm16^{Gt683Lex}$ mutants in and around Meckel's cartilage and the region near the base of the tongue, consistent with the mandibular and salivary gland hypoplasia and gross tongue abnormalities observed in these mutants.

SUPPLEMENTARY FIGURES

Fig. S1

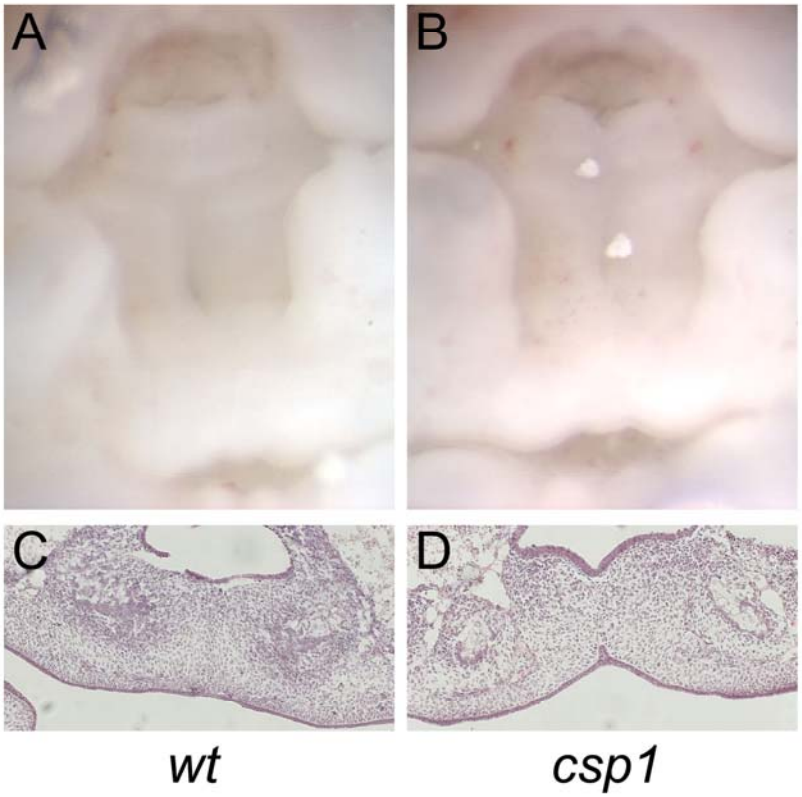

	Shelves Apposed	Shelves Fused	Partial CP	Complete CP
wt (n=25)	23	18	2	0
csp1 (n=10)	8	8	1	1

Fig. S2

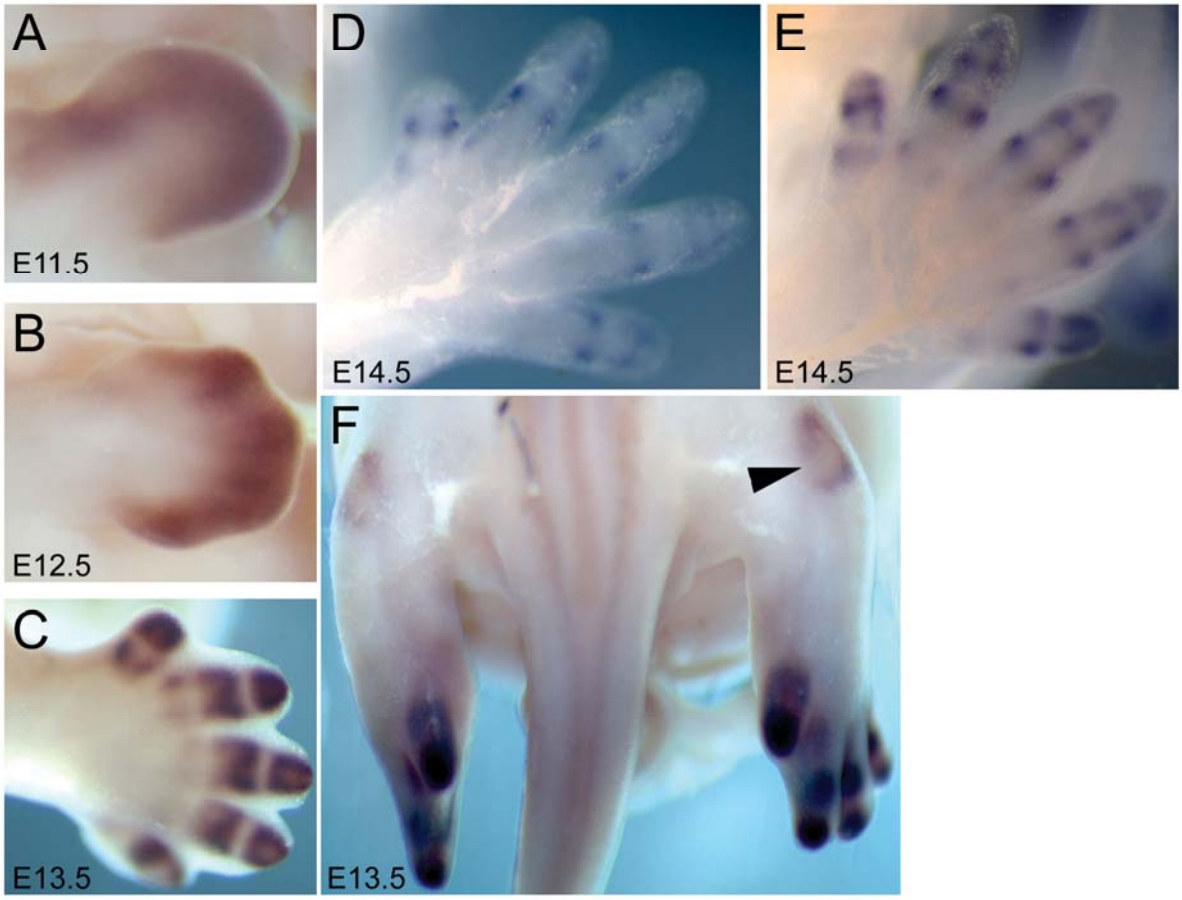

Fig. S3

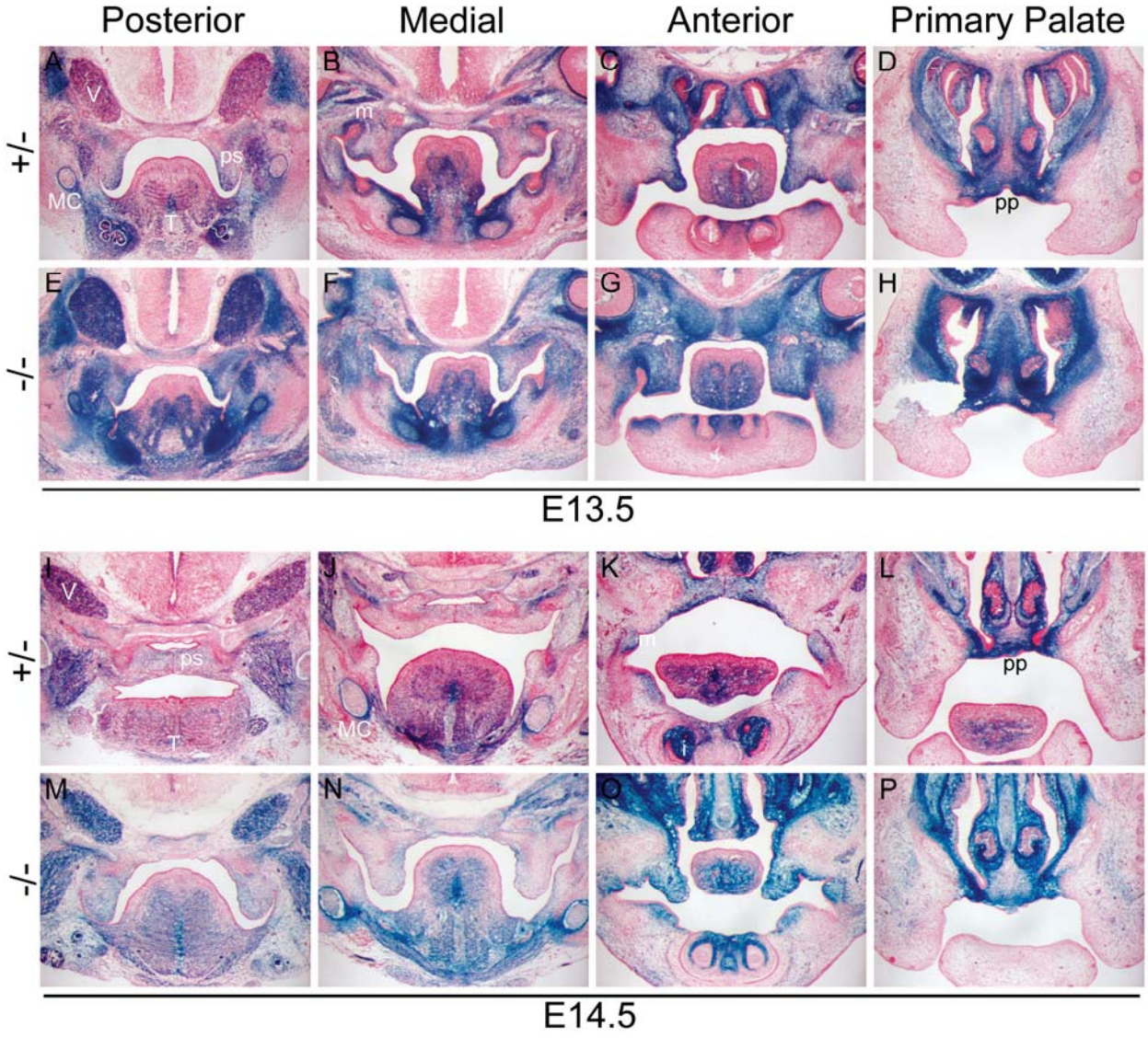
Posterior
Medial
Anterior
Primary Palate
+/-
-/-
A
B
C
D
E
F
G
H
V
ps
MC
T
m
pp
E13.5
I
J
K
L
M
N
O
P
E14.5

Fig. S4

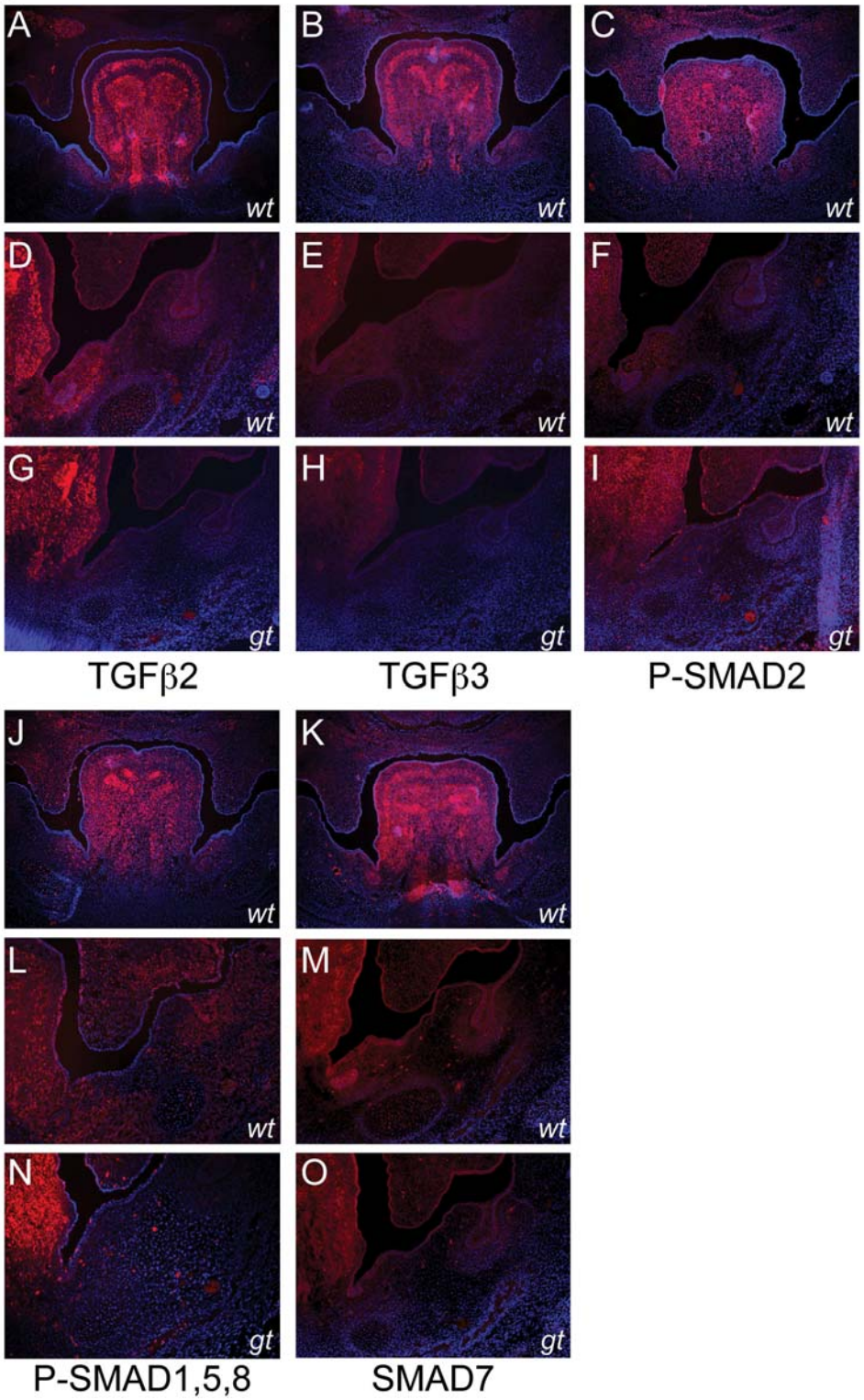
A
wt
B
wt
C
wt
D
wt
E
wt
F
wt
G
gt
H
gt
I
gt
TGFβ2
TGFβ3
P-SMAD2
J
wt
K
wt
L
wt
M
wt
N
gt
O
gt
P-SMAD1,5,8
SMAD7